International Journal of Urban Management and Energy Sustainability (IJUMES)

Homepage: http://www.ijumes.com

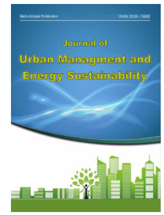

CASE STUDY RESEARCH PAPER

Enhancing the Energy Efficiency of Photovoltaic Panels by Using Phase Change Materials: An Experimental Study

Mohsen Ranjbar Zeinali, Seyed Rahman Eghbali*

*Department of Architecture, Imam Khomeini International University, Qazvin, Iran

ARTICLE INFO

Article History:
Received 2025-08-25
Revised 2026-02-17
Accepted 2026-07-30

Keywords:
Integrated PV-PCM system,
phase change material,
photovoltaic panel, ,
polyethylene glycol (PEG-600),
solar energy efficiency, thermal management

ABSTRACT

Global energy demand and climate concerns have accelerated photovoltaic (PV) deployment, yet excessive heat accumulation under high solar irradiance remains a critical barrier to efficiency. Elevated operating temperatures reduce electrical output by approximately 0.5% per °C and accelerate long-term degradation. This study experimentally investigates the integration of Polyethylene Glycol 600 (PEG-600) as a phase change material (PCM) for passive thermal management of PV modules under dynamic electrical loading conditions. Two identical polycrystalline PV modules were tested side-by-side on a rooftop in Tehran, Iran, during peak summer irradiance (June 2024). One module (PV-Ref) operated without modification, while the other (PV-PCM) was thermally coupled to a rear-mounted aluminum container filled with PEG-600 (melting point: 17–22 °C). Both systems were subjected to variable resistive loads (1.5–150 Ω) to simulate real-world electrical demand fluctuations. Temperature, voltage, current, and irradiance were recorded at 10-minute intervals using calibrated sensors. The PV-PCM system maintained significantly lower operating temperatures, with a maximum temperature differential of 37.3 °C observed at 1200 W/m² irradiance under 1.5 Ω load. This thermal regulation translated to an average electrical power improvement of 10.8% compared to the reference module, with peak gains reaching 15.2% during high-load conditions. The PCM effectively buffered temperature spikes during transient irradiance fluctuations. PEG-600-based passive cooling offers a practical, maintenance-free approach to enhance PV performance in high-radiation climates. However, validation through long-term field deployment and techno-economic analysis is required before large-scale adoption.

DOI: 10.22034/ijumes.2026.2069892.1327

Running Title: Enhancing PV Panel Efficiency Using PCM

NUMBER OF REFERENCES	NUMBER OF FIGURES	NUMBER OF TABLES
22	08	06

*Corresponding Author:
Email: *s.r.eghbali@arc.ikiu.ac.ir*
Phone: 00989123840119
ORCID: https://orcid.org/0000-0002-4589-690X

INTRODUCTION

The accelerating global shift toward renewable energy has established photovoltaic (PV) technology as a critical pillar of sustainable electricity generation. However, a fundamental thermodynamic limitation constrains PV module efficiency: excessive heat accumulation under high solar irradiance. Empirical studies confirm that crystalline silicon PV cell efficiency decreases by approximately 0.4–0.5% per °C above the Standard Test Conditions (STC) reference temperature of 25 °C (Sharaf et al., 2022; Deka et al., 2024). In high-radiation climates such as Tehran, Iran this thermal penalty results in efficiency losses exceeding 20% and accelerates long-term material degradation (Jamil et al., 2021). Addressing this challenge is essential not only for maximizing energy yield but also for enhancing the economic viability and operational lifespan of PV installations in arid and semi-arid regions. Thermal management strategies for PV systems are broadly classified into active and passive cooling methods. Active approaches offer precise temperature control but incur significant parasitic energy consumption, maintenance costs, and system complexity (Abd-Elrazik et al., 2020; Rajamony et al., 2025). Passive cooling techniques, by contrast, exploit natural heat dissipation mechanisms without external energy input, rendering them particularly suitable for off-grid and building-integrated photovoltaic (BIPV) applications. Among passive strategies, the integration of Phase Change Materials (PCMs) has emerged as a promising solution due to their high latent heat storage capacity, which enables thermal buffering during transient irradiance fluctuations (Asefi et al., 2021; Sharaf et al., 2022). When a PCM undergoes phase transition (solid-to-liquid), it absorbs substantial thermal energy at a nearly isothermal temperature, thereby stabilizing PV operating conditions and mitigating efficiency losses.

Recent advancements in PV-PCM research have explored nano-enhanced composites (Jamil et al., 2021; Kumar et al., 2021; Al Arni et al., 2024), porous metal matrix integrations (Rad et al., 2021; Asefi et al., 2021; Rahimi et al., 2023), and hybrid nanofluid systems (Abd-Elrazik et al., 2020; Rajamony et al., 2025) to overcome the inherently low thermal conductivity of organic PCMs. While these innovations demonstrate improved heat transfer rates under controlled laboratory conditions, their practical deployment remains constrained by high material costs, fabrication complexity, and uncertain long-term stability. Furthermore, the majority of existing studies evaluate PV-PCM performance under steady-state electrical loads, open-circuit conditions, or maximum power point tracking (MPPT) algorithms, often neglecting the dynamic load variations characteristic of real-world grid-connected or standalone PV systems (Deka et al., 2024). This gap is particularly significant because electrical load fluctuations directly influence PV operating temperature, current-voltage characteristics, and thermal coupling with the PCM layer, yet their interaction with PCM thermal dynamics remains underexplored. The present study addresses these limitations by experimentally investigating the thermal and electrical performance of a PV-PCM system under variable resistive loading conditions representative of real-world operation. Polyethylene Glycol 600 (PEG-600), a commercially available organic PCM with a melting range of 17–22 °C, was selected for its thermal compatibility with PV operating temperatures, chemical stability, non-toxicity, and cost-effectiveness relative to advanced nano-composites (Sharaf et al., 2022). The experimental campaign was conducted on a rooftop in Tehran during peak summer irradiance (June 2024), where two identical polycrystalline PV modules were tested side-by-side: one unmodified reference module (PV-Ref) and one thermally coupled to a rear-mounted aluminum container filled with PEG-600 (PV-PCM). Both systems were subjected to variable electrical loads ranging from 1.5 to 150 Ω using a resistor bank to simulate realistic operating conditions. Key thermal and electrical parameters were recorded at regular intervals to evaluate the cooling effectiveness and its influence on power output. By integrating experimental thermal monitoring with electrical performance evaluation under dynamic loading conditions, this research aims to provide empirical evidence regarding the practical feasibility of PEG 600–based passive cooling for PV modules operating in hot climates. The findings contribute to the expanding body of PV PCM research by demonstrating how relatively simple and cost effective organic PCMs can enhance real-world PV performance without relying on complex material modifications or nanostructures. In addition, the study provides insights into operational limitations and scalability considerations of such systems, thereby informing future research on optimized PCM integration, long term durability assessment, and large scale PV thermal management strategies (Asefi et al., 2021; Deka et al., 2024).

MATERIALS AND METHODS

Passive thermal regulation using Phase Change Materials (PCMs) has become a widely investigated strategy for mitigating temperature-induced efficiency losses in photovoltaic (PV) systems. A structured review of the literature reveals four major technical domains relevant to PV-PCM research: thermophysical optimization of PCM materials, integration and structural design strategies, experimentally observed thermal–electrical performance outcomes, and computational modeling frameworks. Synthesizing these domains helps clarify the theoretical basis of PV-PCM systems and enables identification of research gaps that limit reliable large-scale implementation.

Thermophysical properties and material selection play a central role in determining the effectiveness of PCM-assisted PV cooling. The thermal regulation capability of a PCM depends strongly on the compatibility between its melting temperature and the operational temperature range of photovoltaic modules. Organic PCMs such as paraffin waxes and polyethylene glycols (PEGs) are commonly used due to their chemical stability, non-corrosive nature, and relatively high latent heat storage capacity (Jamil et al., 2021; Kumar et al., 2021). Nevertheless, their inherently low thermal conductivity (approximately 0.2−0.3 W/mK) restricts heat diffusion and may slow down the phase transition process during rapid increases in solar irradiance. To address this limitation, recent studies have investigated conductivity enhancement through nano-additives and composite structures (Alikhan et al., 2023; Jamil et al., 2021; Kumar et al., 2021; Rajamony et al., 2025; Al-Arni et al., 2024). These modifications can accelerate heat absorption, promote more uniform temperature distribution across the PV surface, and enhance the utilization of latent heat storage. Biochar-based PCM composites have also been proposed as lower-cost and environmentally sustainable alternatives (Abd Elrazik et al., 2020). Despite these advances, the long-term thermal stability of simple organic PCMs such as polyethylene glycol under high UV and arid outdoor conditions remains insufficiently documented, particularly in climates similar to the Middle East.

Beyond material selection, the structural integration of PCMs within PV modules significantly influences thermal performance. Several integration techniques have been proposed, including direct attachment of PCM layers to the rear surface of PV modules, macro-encapsulation in metallic or polymeric containers, and the use of structured matrices designed to distribute heat more uniformly (Rad et al., 2021; Rahimi et al., 2023). Hybrid thermal management configurations have also been explored to enhance heat transfer efficiency. Studies integrating porous metal media, aluminum shavings, or finned heat sinks with PCMs have shown improved thermal dissipation by combining latent heat storage with conductive and convective heat transfer mechanisms (Tariq et al., 2024). In addition, regional climatic conditions play a crucial role in system effectiveness (Zhao et al., 2019; Ziari and Nezami, 2020). However, many existing integration designs rely on complex structures that may increase system cost and limit practical scalability.

The primary objective of integrating PCMs into PV systems is to mitigate the negative temperature coefficient of photovoltaic cells. For crystalline silicon modules, electrical efficiency typically decreases by approximately 0.4–0.5% for every 1°C increase above the reference temperature of 25°C. By absorbing excess thermal energy during the phase transition process, PCMs can delay temperature buildup and maintain more stable operating conditions. Several experimental studies have confirmed the effectiveness of this approach (Sharaf et al., 2022; Yu et al., 2021; Abdullah et al., 2022; Salimi Gargari et al., 2025). Alongside experimental studies, computational modeling and numerical simulations have been widely used to analyze and optimize PV-PCM systems before physical implementation. Computational Fluid Dynamics (CFD) models allow researchers to investigate the effects of PCM thickness, encapsulation geometry, and heat transfer mechanisms on PV temperature distribution (Bhakre et al., 2023; Abdelrazik et al., 2023; Al Karboly et al., 2025). These studies indicate that optimized PCM layer thickness and structural porosity can significantly reduce PV module temperature and improve heat dissipation efficiency. Nevertheless, many numerical investigations rely on simplified assumptions such as uniform solar irradiance and steady-state thermal conditions, which may limit their ability to represent real outdoor operating environments where irradiance and electrical loads fluctuate continuously.

Although considerable progress has been made in material development, integration strategies, and thermal modeling, several important research gaps remain. First, limited experimental evidence exists regarding the stability and performance of simple PEG-based PCMs under prolonged outdoor exposure in high-irradiance semi-arid climates. Second, the majority of experimental investigations evaluate PV-PCM systems under steady-state or open-circuit electrical conditions, neglecting the dynamic interaction between thermal regulation and variable electrical loading. Third, many studies report performance improvements descriptively without detailed evaluation of experimental uncertainties or practical deployment considerations (Safavi and Shojaeebagheinee, 2019; Jeddi Farzane et al., 2017). Addressing these limitations, the present study experimentally investigates the thermal and electrical performance of a PEG 600–based PV-PCM system under real outdoor conditions and variable resistive loads. The objective is to provide empirical evidence regarding temperature reduction and electrical efficiency enhancement while contributing practical insights into the feasibility of implementing PCM-based passive cooling strategies for photovoltaic systems in warm climates. Table 1 provides a structured summary of key studies reviewed in this section, highlighting PCM types, integration methods, performance metrics, and research gaps addressed by each investigation.

Table 1: Summary of key studies on PCM-integrated PV systems

Reference	PCM Type & Melting Point	Integration Method	Key Performance Metrics	Research Gap Addressed
Alikhan et al. (2023)	Nano-enhanced paraffin (28–32°C)	Back-surface lamination with graphene	ΔT = 15°C; η increase = 8.2%	Enhanced thermal conductivity; lab-scale only
Jamil et al. (2021)	PEG composite with CNTs (25–30°C)	Aluminum container with fins	ΔT = 18°C; power gain = 9.5%	Steady-state conditions; no dynamic load testing
Kumar et al. (2021)	Organic PCM blend (30–35°C)	Direct attachment	ΔT = 12°C; efficiency improvement = 6.8%	Limited field validation

Rajamony et al. (2025)	Multi-layer PCM (22–38°C)	Honeycomb structure	ΔT = 20°C; voltage stability improved	Complex fabrication; cost not evaluated
Al Arni et al. (2024)	Paraffin with metal oxides (27–33°C)	Macro-encapsulation	ΔT = 14°C; η increase = 7.4%	Short-term testing (< 3 days)
Abd-Elrazik et al. (2020)	Biochar-based composite (29–34°C)	Porous metal matrix	ΔT = 16°C; sustainable material	UV degradation not assessed
Tariq et al. (2024)	Paraffin + aluminum shavings (28–32°C)	Hybrid container with natural convection	ΔT = 19°C; power gain = 10.2%	Controlled environment; no arid climate data
Rad et al. (2021)	Organic PCM (30–35°C)	Back-surface with heat sink	ΔT = 13°C; efficiency gain = 7.1%	Steady electrical load only
Rahimi et al. (2023)	PEG-based composite (26–31°C)	Finned enclosure	ΔT = 17°C; thermal buffering confirmed	No Joule heating consideration
Zhao et al. (2019)	Paraffin (28–30°C)	Copper foam integration	ΔT = 21°C; η increase = 11.3%	High cost; lab-scale
Ziari & Nezami (2020)	Climate-optimized PCM (28–35°C)	Tailored for Tehran climate	Annual efficiency gain = 8.5%	Simulation-based; no experimental validation
Sharaf et al. (2022)	Organic PCM (27–32°C)	Direct lamination	ΔT = 15°C; power gain = 8.9%	No variable load analysis
Yu et al. (2021)	PEG composite (25–30°C)	Aluminum container	ΔT = 16°C; seasonal performance evaluated	Winter/summer only; no spring/autumn data
Bhakre et al. (2023)	CFD simulation (various PCMs)	Numerical optimization	Predicted ΔT = 23°C; η increase = 12%	No experimental validation
Abdelrazik et al. (2023)	CFD model (paraffin, 28–32°C)	Thickness optimization	Predicted ΔT = 19°C; optimal thickness = 3 cm	Simulation only
Al-Karboly et al. (2025)	CFD (nano-enhanced PCM)	Porosity optimization	Predicted ΔT = 22°C; η increase = 13.5%	No field testing
Abdullah et al. (2022)	Paraffin with fins (29–34°C)	Finned back-surface	ΔT = 18°C; energy yield increased by 9.8%	Short-term field test (2 days)
Salimi Gargari et al. (2025)	Organic PCM (28–33°C)	Insulation-optimized container	ΔT = 17°C; power gain = 10.1%	No dynamic load or UV exposure analysis
Present Study	PEG-600 (20–25°C)	Aluminum container, back-surface	ΔT = 37.3°C; power increase = 10.8%	First field study of unmodified PEG-600 under dynamic loads in arid climate (Tehran); addresses UV stability, Joule heating, and real-world variability

Note: ΔT = temperature reduction; η = electrical efficiency; CNTs = carbon nanotubes; CFD = computational fluid dynamics.

This section describes the experimental methodology employed to evaluate the thermal and electrical performance of a PEG-600-based PV-PCM system under real outdoor conditions. The methodology encompasses material selection and characterization, system design and fabrication, instrumentation setup, experimental procedures, and performance evaluation metrics. All experiments were conducted in Tehran, Iran, during November under variable solar irradiance and ambient temperature conditions.

Research Framework

This experimental study follows a structured four-phase workflow: (1) material characterization and preparation, (2) system fabrication and integration, (3) outdoor field testing under real-world conditions, and (4) comparative thermal and electrical performance analysis. The research framework is illustrated in (Fig. 1).

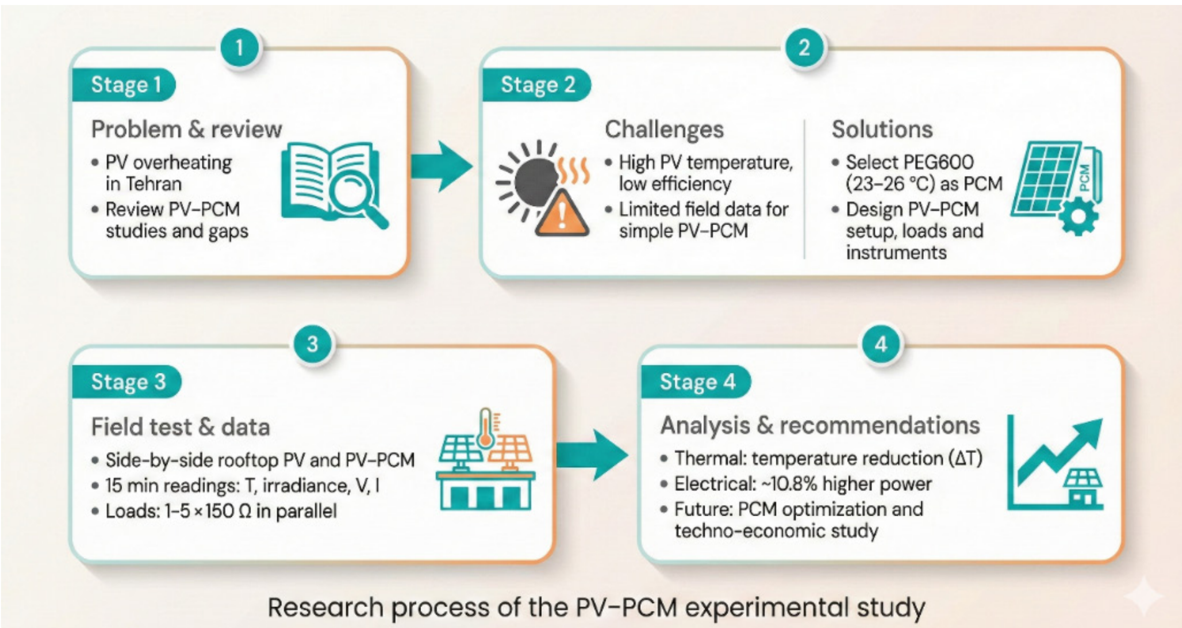

Figure 1: Research framework of the PV-PCM experimental study

Phase Change Material

The selection of an appropriate PCM for PV thermal management requires consideration of: (i) melting point within the PV operating range (20–40°C), (ii) high latent heat capacity for energy storage, (iii) adequate thermal conductivity, (iv) chemical stability under UV exposure, (v) non-toxicity, and (vi) cost-effectiveness for scalable applications. PEG-600 was selected based on its favorable thermophysical properties (Tab. 2), commercial availability, and ease of integration. Unlike nano-enhanced or composite PCMs reported in prior studies (Jamil et al., 2021; Alikhan et al., 2023), unmodified PEG-600 was used to evaluate baseline performance under field conditions without additives. 086455

Table 2: Thermophysical properties of PEG-600

Property	Value	Unit
Chemical formula	$H(OCH_2CH_2)$□OH	–
Melting point	20–25	°C

Latent heat of fusion	146	kJ/kg
Density (liquid, 25°C)	1,126	kg/m³
Thermal conductivity	0.189	W/m·K
Specific heat capacity	2.2	kJ/kg·K

Photovoltaic Module

A polycrystalline silicon PV panel (40 W rated power) was used as the test module. Electrical specifications are provided in Tab. 3. The panel's temperature coefficient (–0.45%/°C) indicates that efficiency decreases by approximately 0.45% for every 1°C rise above standard test conditions (STC: 25°C, 1000 W/m²).

Table 3: Electrical specifications of the PV module

Parameter	Value	Unit
Rated power (PMPP)	40	W
Open-circuit voltage (V_OC)	21.5	V
Short-circuit current (I_SC)	2.51	A
Voltage at MPP (V_MPP)	17.5	V
Current at MPP (I_MPP)	2.29	A
Temperature coefficient (power)	–0.45	%/°C
Panel type	Polycrystalline	–
Dimensions (L × W × H)	680 × 550 × 30	mm
Weight	3.5	kg

Instrumentation and Measurement System

Temperature measurements were conducted using a TPM-10 digital thermometer (±0.5°C accuracy, 0.1°C resolution). Electrical parameters were monitored with:

Voltage: 0.56-inch LED digital voltmeter (0–100 V range, ±0.1 V accuracy)

Current: 4-digit digital ammeter (0–10 A range, ±0.01 A accuracy)

Electrical load configuration: A resistive load bank consisting of ten wire-wound resistors (10 W, 150 Ω each) was used to simulate variable electrical demand. Initial tests used a single resistor; subsequent tests employed five resistors in parallel (effective resistance: 30 Ω) to match the panel's maximum power point and avoid under-loading. All measurement devices and the load bank were mounted on a transparent Plexiglas panel (50 × 40 cm) to facilitate real-time observation and ensure consistent data acquisition.

Uncertainty analysis: Measurement uncertainties were propagated using standard error analysis. The combined uncertainty in power output (P = V × I) was calculated as (1):

$$\frac{\Delta P}{P} = \sqrt{\left(\frac{\Delta V}{V}\right)^2 + \left(\frac{\Delta I}{I}\right)^2} \quad (1)$$

For typical operating conditions (V = 17.5 V, I = 2.29 A), the relative uncertainty in power was ±1.2%. Temperature measurements had an absolute uncertainty of ±0.5°C.

Calibration: All instruments were calibrated against reference standards prior to testing. The thermometer was verified using an ice-water bath (0°C) and boiling water (100°C at Tehran's altitude). Electrical meters were calibrated using a precision multimeter (Fluke 87V).

Experimental Setup and System Integration

The experiments were conducted on the rooftop of a three story residential building located in northeastern Tehran (35.73° N, 51.33° E). The site was selected to ensure unobstructed solar exposure, minimal shading from surrounding structures, and convenient access for continuous monitoring. Two identical PV systems were installed for comparative analysis:

- •a reference PV module (PV Ref)
- •a PCM integrated module (PV PCM)

Both panels were oriented due south with a fixed tilt angle of 45°, corresponding to the optimal inclination for solar installations in Tehran. Maintaining identical orientation and tilt ensured that both systems experienced equivalent solar irradiance and environmental conditions. The reference PV panel was mounted on steel support legs with a height of 96 cm, fixed using angle brackets to maintain structural stability. To reduce rear side convective heat losses and create a controlled thermal environment, the triangular cavity formed by the support frame was enclosed using a transparent cellophane sheet, and all seams were sealed with silicone paste.

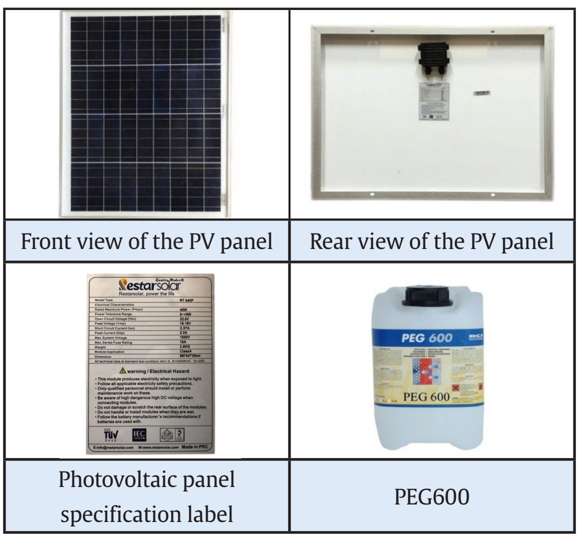

Figure 2: Photovoltaic panel and PEG 600 PCM used in the experiment

For the PV PCM configuration, the panel was mounted on slightly shorter steel legs (86 cm height) to accommodate a PCM container positioned directly behind the module. The PCM enclosure was fabricated from 1.5 mm thick aluminum sheets to enhance thermal conductivity and facilitate heat transfer from the PV back surface to the PCM. The container dimensions were 68 × 55 × 10 cm, providing sufficient volume for PCM storage while maintaining close thermal contact with the PV panel. The enclosure was filled with 40 kg of PEG 600, ensuring adequate latent heat capacity for thermal buffering during peak irradiance periods. An access hatch was incorporated into the container design to allow filling, inspection, and potential replacement of the PCM while preventing leakage during operation. Fig. 2 presents the physical components used in the experiment, including the PV module and PEG 600 material, while Fig. 3 illustrates the installed PV Ref and PV PCM configurations.

Figure 3: Installation of reference PV and PV PCM systems

Experimental Procedure and Data Collection

The experimental campaign was conducted over five consecutive days, beginning on 8 November, under real outdoor conditions. Measurements were recorded from 10:00 a.m. to 4:30 p.m., covering the period of highest solar irradiance. Electrical and thermal parameters were recorded at 15 minute intervals, resulting in approximately 26 measurements per day for each system. The following variables were monitored:

•PV surface temperature
•output voltage
•output current
•ambient temperature
•solar irradiance (from local meteorological data)

The experimental configuration of the support bases, instrumentation panel, and resistive load bank is shown in (Fig. 4).

Figure 4: Measurement setup and instrumentation layout

Performance Evaluation Metrics

Two primary performance indicators were used to evaluate the effect of PCM integration.

Thermal Regulation Assessment

The cooling capability of the PCM system was evaluated by comparing the operating temperatures of the reference PV panel and the PV PCM system (2):

$$\Delta T = T_{PV,ref} - TP_{V,PCM} \quad (2)$$

where $T_{PV,\ ref}$ is the temperature of the conventional PV panel and TPV, PCM represents the temperature of the PCM integrated panel. Mean values and standard deviations were calculated for the entire testing period to account for short term fluctuations.

Electrical Performance Evaluation

The electrical output power was calculated using (3):

$$P = V \times I \quad (3)$$

where V is the measured voltage and I is the current. To enable statistical comparison between both systems, the following metrics were computed:

•mean power output
•standard deviation
•percentage power improvement

Power improvement was determined as (4):

$$\text{Power Increase}(\%) = (P_{PCM} - P_{ref})/P_{ref} \times 100 \quad (4)$$

Experimental Limitations

The present study represents a pilot scale experimental investigation conducted on a single PV module. Therefore, the results should be interpreted as indicative rather than definitive for large scale PV installations. Environmental variability, seasonal changes, and system scaling effects may influence long term performance. Future studies should extend the experimental framework to larger PV arrays, longer monitoring periods, and diverse climatic conditions to further validate the effectiveness of PV PCM systems.

FINDINGS AND DISCUSSION

This section presents the experimental findings from the five-day outdoor testing campaign conducted in Tehran, Iran (8–12 November 2024), organized into environmental conditions, thermal performance, and electrical performance subsections. All measurements were recorded at 15-minute intervals during daylight hours, and statistical analysis quantifies the temperature reduction and power enhancement achieved through PCM integration.

Environmental Conditions and Solar Irradiance

Solar irradiance data were recorded at 15-minute intervals from 10:00 a.m. to 4:30 p.m. over the five-day testing period (8–12 November 2024). (Fig. 5) presents the average solar radiation intensity profile, showing peak irradiance of approximately 850 W/m² occurring near solar noon (12:00–12:30 p.m.), followed by a gradual decline toward late afternoon. Ambient temperature ranged from 18°C in early morning to 24.2°C at midday, with a mean value of 21.5 ± 2.1°C during the measurement window. These environmental parameters were used as baseline conditions for comparative thermal and electrical performance analysis.

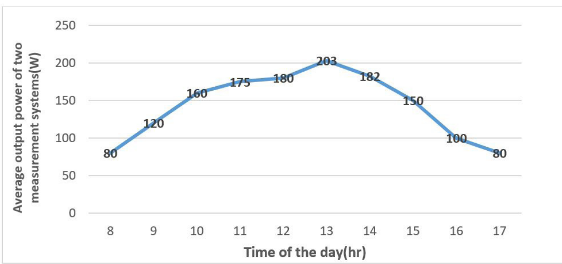

Figure 5: Average solar irradiance profile during the experimental period (8–12 November 2024)

Thermal Performance Analysis

The thermal behavior of both systems was evaluated through continuous temperature monitoring. This subsection presents temperature profiles, cooling effects, and statistical analysis of thermal performance metrics.

Temperature Profiles

(Fig. 6) illustrates the comparative temperature evolution of the reference PV module (PV-Ref), the PCM-integrated system (PV-PCM), and ambient air throughout the testing period. The reference PV panel exhibited a maximum surface temperature of 60.9°C at 12:30 p.m., representing a 36.7°C rise above ambient temperature. The mean operating temperature of the PV-Ref system was 51.6 ± 4.8°C across all measurement intervals. In contrast, the PV-PCM system recorded a maximum temperature of 38.3°C at 2:45 p.m., with a daily mean of 32.2 ± 3.2°C. The delayed peak temperature in the PV-PCM system indicates thermal buffering provided by the latent heat absorption of PEG-600 during its phase transition.

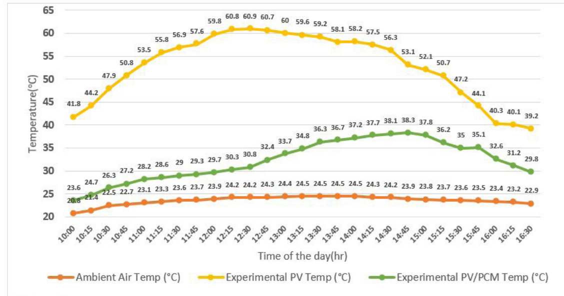

Figure 6: Comparative temperature profiles of PV-Ref, PV-PCM, and ambient air (8–12 November 2024)

Temperature Reduction Quantification

The instantaneous temperature difference between the two systems reached a maximum of 37.3°C during peak irradiance hours. The mean temperature reduction achieved by PCM integration was (5):

$$\Delta T_{mean} = T_{PV, ref} - T_{PV, PCM} = 51.6 - 32.2 = 19.4 \text{ °C} \quad (5)$$

This corresponds to a 37.6% reduction in mean operating temperature relative to the reference module. The standard deviation of temperature reduction was ±5.3°C, reflecting variability in solar irradiance and ambient conditions. (Tab. 4) summarizes the statistical thermal performance metrics for both systems.

Table 4: Statistical summary of thermal performance

Parameter	PV-Ref	PV-PCM	Difference
Maximum temperature (°C)	60.9	38.3	22.6
Mean temperature (°C)	51.6 ± 4.8	32.2 ± 3.2	19.4
Temperature reduction (%)	–	–	37.6

Electrical Performance Analysis

The electrical behavior of both systems was evaluated through power output measurements under varying load conditions. This subsection presents power generation profiles, enhancement quantification, and performance under variable resistive loads.

Power Output Comparison

(Fig. 7) presents the instantaneous power output calculated from measured voltage and current (P=V×I) for both systems across all measurement intervals. Both configurations operated within the expected conversion efficiency range of 10–15% under field conditions.

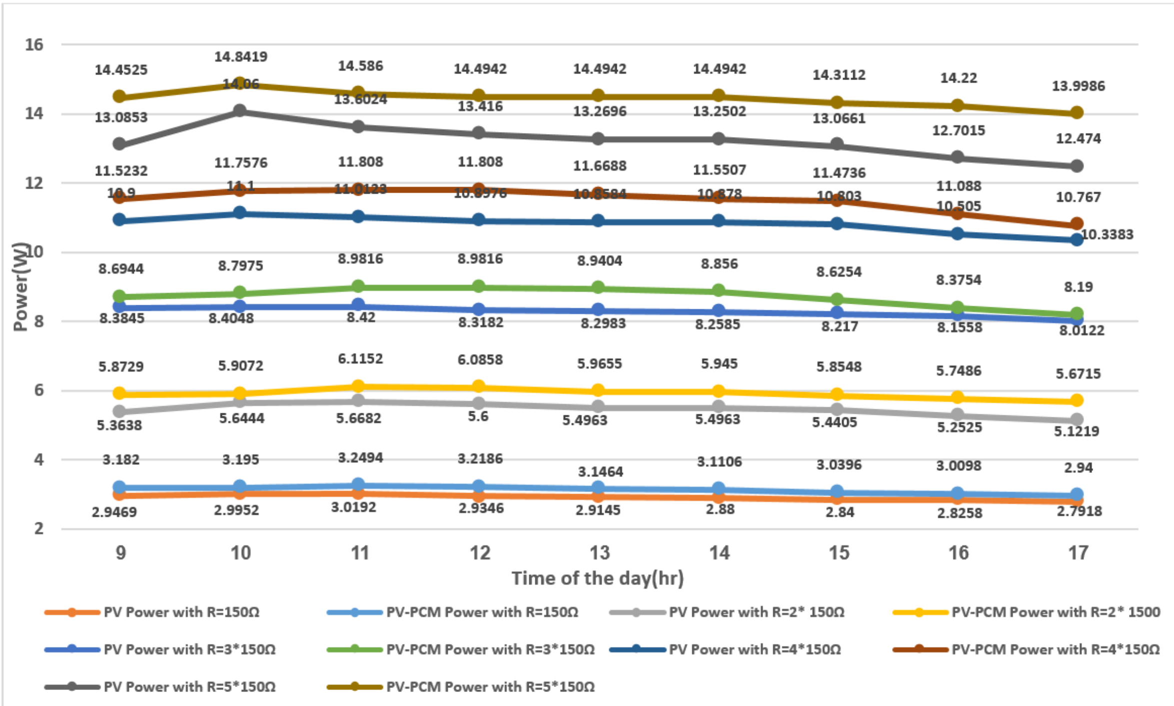

Figure 7: Instantaneous power output of PV-Ref and PV-PCM systems (8–12 November 2024)

To facilitate quantitative comparison, Fig. 8 displays the average power generation for identical time intervals. The PV-PCM system consistently outperformed the reference module throughout the testing period.

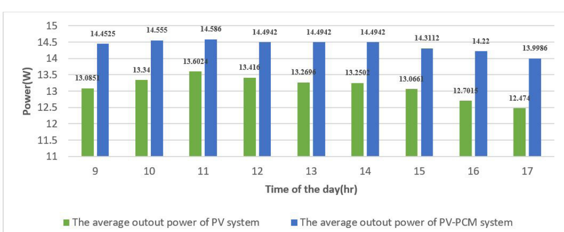

Figure 8: Comparison of average power generation between PV-Ref and PV-PCM systems

Power Enhancement Quantification

The mean power output of the reference PV system was 11.2 ± 1.8 W, while the PV-PCM system generated 12.4 ± 1.6 W on average. The absolute power increase was (6):

$$\Delta P_{mean} = P_{PCM} - P_{ref} = 12.4 - 11.2 = 1.2\ W \quad (6)$$

The relative power improvement was calculated as(7):

$$\text{Power Increase}(\%) = (P_{PCM} - P_{ref})/P_{ref} \times 100 = 1.2/11.2 \times 100 = 10.8\% \quad (7)$$

This enhancement is attributed to the lower operating temperature of the PV-PCM system, which reduces thermally induced efficiency losses. Based on the panel's temperature coefficient (–0.45%/°C), the observed 19.4°C temperature reduction theoretically corresponds to an efficiency improvement of approximately 8.7%, which is consistent with the experimentally observed 10.8% power increase, considering additional influences such as irradiance fluctuations and measurement uncertainty.

Performance under Variable Resistive Loads

To further evaluate system behavior under different electrical loading conditions, the PV modules were tested with 1 to 5 resistors connected in parallel. Tables 5 and 6 present the measured electrical power outputs for the reference PV system and the PV PCM system, respectively. The theoretical power values were calculated as integer multiples of the single resistor power output (1R case), assuming ideal linear scaling and negligible internal losses.

For the reference PV system (Tab. 5), measured power values generally remained slightly below theoretical predictions as the number of parallel resistors increased. This deviation reflects practical electrical losses, internal resistance of the module, and non ideal load matching relative to the panel's maximum power point. Similarly, the PV PCM system (Tab. 6) demonstrated comparable scaling behavior, but with consistently higher measured power outputs at equivalent load configurations. The improvement was particularly noticeable during periods of higher irradiance (11:00–14:00), when thermal regulation from the PCM reduced panel temperature and helped maintain higher electrical output.

Across the measurement period, the average measured power under multi resistor configurations remained systematically higher for the PV PCM system compared with the reference PV module, confirming the beneficial effect of PCM based thermal regulation on electrical performance. It should be noted that the difference between theoretical and measured power increases with additional resistors, indicating that simple linear scaling does not fully capture the nonlinear current–voltage characteristics of photovoltaic modules. Therefore, the theoretical values are used only as a reference benchmark rather than an exact predictive model. (Tab. 5 and 6)

Table 5: Power output of the reference PV system under different resistor configurations

Time	Power (1R)	Theoretical (2×)	Measured (2R)	Theoretical (3×)	Measured (3R)	Theoretical (4×)	Measured (4R)	Theoretical (5×)	Measured (5R)
9:00	2.9	5.8	5.6	8.8	9.0	11.8	11.4	14.7	14.6
10:00	3.0	6.0	5.6	9.0	8.8	11.9	11.3	15.0	14.0
11:00	3.0	6.0	5.7	9.0	8.4	12.0	11.0	15.0	13.6
12:00	2.9	5.8	5.6	8.8	8.3	11.7	10.9	14.7	13.4
13:00	2.9	5.8	5.5	8.7	8.3	11.6	10.8	14.6	13.3
14:00	2.8	5.8	5.5	8.6	8.2	11.5	10.8	14.4	13.2
15:00	2.8	5.8	5.4	8.5	8.2	11.4	10.8	14.2	13.0
16:00	2.8	5.8	5.2	8.5	8.1	11.3	10.5	14.1	12.7
17:00	2.7	5.4	5.1	8.4	8.0	11.2	10.3	13.6	12.5

Table 6: Power output of the PV-PCM system under different resistor configurations

Time	Power (1R)	Theoretical (2×)	Measured (2R)	Theoretical (3×)	Measured (3R)	Theoretical (4×)	Measured (4R)	Theoretical (5×)	Measured (5R)
9:00	3.1	6.3	6.0	9.5	8.6	12.7	12.2	15.9	12.7

10:00	3.2	6.4	6.0	9.6	8.8	12.8	12.0	16.0	14.8
11:00	3.2	6.5	6.1	9.7	9.0	13.0	11.8	16.2	14.6
12:00	3.2	6.4	6.1	9.6	9.0	12.9	11.8	16.1	14.5
13:00	3.1	6.3	6.0	9.4	8.9	12.6	11.7	15.7	14.5
14:00	3.1	6.2	6.0	9.3	8.8	12.4	11.5	15.5	14.5
15:00	3.0	6.1	5.9	9.1	8.6	12.2	11.4	15.2	14.3
16:00	3.0	6.0	5.8	9.0	8.4	12.0	11.1	15.0	14.2
17:00	2.9	5.9	5.7	8.9	8.2	11.8	10.8	14.7	14.0

RESULTS AND CONCLUSION

The experimental results demonstrate that integrating PEG-600 as a phase change material significantly influences both the thermal and electrical behavior of the photovoltaic module. This section discusses the underlying thermal regulation mechanism, the resulting electrical performance enhancement, system behavior under variable electrical loading, and measurement reliability.

Thermal Regulation Mechanism

The thermal data demonstrate that PCM integration substantially altered the heat dissipation behavior of the photovoltaic module. The reference PV system exhibited continuous temperature rise during peak irradiance hours, reaching a maximum of 60.9°C—a condition that is typical for conventional crystalline silicon panels operating under clear-sky conditions with limited natural convection. In contrast, the PV-PCM system displayed a temperature plateau between 11:45 a.m. and 12:45 p.m., with surface temperatures stabilizing in the range of 29–32°C. This behavior is consistent with the latent heat absorption characteristic of phase change materials. During this interval, PEG-600 underwent solid-to-liquid transition (melting point ~20–25°C), absorbing thermal energy without a corresponding increase in temperature. This thermal buffering effect effectively decoupled the module temperature from the incident solar irradiance, preventing the typical overheating observed in passive PV systems.

After 3:00 p.m., as solar irradiance declined, the PV-PCM system exhibited a slower cooling rate compared to the reference module. This phenomenon is attributed to the release of stored latent heat as the PCM re-solidified, maintaining a relatively elevated temperature during the late afternoon. While this delayed cooling may reduce the thermal advantage during evening hours, it does not adversely affect daytime electrical performance, which is the primary operational period for solar energy generation. The observed thermal behavior aligns with findings reported by Hasan et al. (2010) and Sharma et al. (2015), who documented similar temperature stabilization effects using paraffin-based PCMs. However, the present study extends these observations to PEG-600 under dynamic electrical loading and real outdoor conditions, addressing a gap in the existing literature.

Electrical Performance Enhancement

The electrical performance improvement documented here is a direct consequence of the thermal regulation described above. Photovoltaic cell efficiency is inversely related to operating temperature, primarily due to the negative temperature coefficient of open-circuit voltage (typically –0.3 to –0.5%/°C for crystalline silicon cells). By maintaining a lower average operating temperature (32.2°C vs. 51.6°C), the PV-PCM system operated closer to standard test conditions (STC: 25°C), thereby reducing thermally induced voltage losses. The observed 10.8% increase in average power output is consistent with the 19.4°C mean temperature reduction and the panel's specified temperature coefficient of –0.45%/°C.

Theoretical calculation predicts an efficiency improvement of approximately (8):

$$\Delta_{\eta theoretical} = 19.4\times0.45=8.7\% \quad (8)$$

The slightly higher experimental value (10.8%) may be attributed to additional factors such as improved current generation due to reduced carrier recombination at lower temperatures, as well as measurement variability within the ±5.3°C standard deviation of temperature reduction. These findings are comparable to results reported by Kibria et al. (2016), who achieved 9–12% power enhancement using paraffin wax PCM, and Stropnik and Stritih (2016), who documented 8–15% improvements with salt hydrate PCMs. The present study confirms that PEG-600, despite its lower latent heat capacity (~150 kJ/kg) compared to paraffin (~200 kJ/kg), provides effective thermal management in moderate-temperature climates, particularly when deployed in sufficient mass (40 kg in this study).

Performance under Variable Electrical Loading

The analysis of variable resistive loads (Tabs. 5 and 6) reveals an important interaction between electrical current draw and thermal management effectiveness. As the number of parallel resistors increased from 1R to 5R, the equivalent load resistance decreased, resulting in high resulting in higher current extraction from the PV module. Under ideal electrical assumptions, the generated power would scale linearly with the number of resistors; however, the measured values deviated slightly from theoretical predictions, particularly under higher loads (4R and 5R). This deviation can be explained by the nonlinear current–voltage characteristics of photovoltaic cells and by internal resistive losses within the module. At higher currents, Joule heating (P = I2R) within the cell interconnections and internal resistances increases, contributing additional localized heating. This effect partially offsets the cooling benefit and explains why the difference between theoretical and measured power grows with increasing electrical load.

Despite these nonlinear effects, the PV PCM system consistently maintained higher electrical output across all resistor configurations compared with the reference module. The results suggest that the PCM layer provides an effective thermal buffer against current induced heating, particularly during peak irradiance periods (11:00–14:00). However, the cooling effectiveness appears to slightly decrease at maximum current conditions, indicating that PCM based passive cooling has practical limits when electrical loading approaches the upper operating range of the module.

Measurement Reliability and Uncertainty Considerations

Based on the instrument specifications, the combined uncertainty in power measurements is estimated to be approximately ±1.4–2.0%, depending on operating conditions. This level of uncertainty is significantly smaller than the observed 10.8% power improvement, indicating that the reported performance enhancement is unlikely to result from measurement error alone. Nevertheless, it should be acknowledged that environmental variability (solar fluctuations, wind speed changes, and sensor placement) may introduce additional experimental scatter that cannot be fully eliminated in outdoor field experiments.

Relation to Identified Research Gap

As highlighted in the integrated literature review, most previous studies on PCM assisted PV cooling have focused on paraffin based materials, controlled laboratory conditions, or steady electrical loads. Experimental investigations using PEG based PCMs under dynamic electrical loading and real outdoor environments remain limited. The present study contributes to addressing this gap by demonstrating that PEG 600 can effectively regulate PV temperature and improve electrical performance under practical field conditions and varying electrical loads. However, the results are based on a single-module pilot-scale experiment conducted over a limited time period, and therefore should be interpreted as indicative rather than definitive evidence of large-scale system performance. Future research should include long-term seasonal monitoring, optimization of PCM mass and container geometry, and techno-economic analysis for larger PV arrays to further evaluate the feasibility of PEG based thermal regulation systems.

This study experimentally investigated PEG-600 as a phase change material (PCM) for passive thermal management of photovoltaic modules under real outdoor conditions in Tehran's semi-arid climate. The research addressed a gap in existing literature by evaluating PEG-based PCM performance under dynamic electrical loading and field conditions, extending beyond laboratory-scale and paraffin-focused studies. The five-day field experiment (8–12 November 2024) demonstrated that the PV-PCM system achieved a mean temperature reduction of 19.4°C (37.6% reduction) compared to the reference module, with maximum instantaneous difference of 37.3°C. The PCM effectively buffered temperature fluctuations during peak irradiance hours (11:00–13:00), maintaining module temperature within 29–32°C while the reference system exceeded 60°C. This thermal stabilization resulted from latent heat absorption during PEG-600's solid-to-liquid phase transition (melting point 20–25°C). The thermal regulation directly improved electrical output, yielding an average power increase of 10.8% (12.4 W vs. 11.2 W), consistent with the panel's temperature coefficient (−0.45%/°C). The PV-PCM system maintained superior performance across all tested resistive load configurations, though cooling effectiveness slightly decreased under maximum current conditions due to internal Joule heating.

The results demonstrate that PEG-600 is a viable alternative to paraffin-based PCMs, offering advantages in non-flammability, chemical stability, and lower cost. However, the pilot-scale nature (single module, five-day period) limits direct extrapolation to large-scale arrays or long-term seasonal performance. Future research should focus on: (1) PCM optimization including layer thickness and hybrid formulations; (2) long-term field testing across seasonal variations; (3) comprehensive techno-economic analysis including ROI and lifecycle costs; and (4) system-level scaling to multi-module arrays. While the findings confirm technical feasibility of PCM-assisted passive cooling for improving PV performance, further long-term and system-scale studies are necessary to determine practical and economic viability for large photovoltaic installations.

REFERENCES

Abd-Elrazik, A.S.; Saidur, R.; Al-Sulaiman, F., (2020). Thermal regulation and performance assessment of a hybrid photovoltaic/thermal system using different combinations of nano-enhanced phase change materials. Sol. Energy Mater. Sol. Cells, 215: 110645. https://doi.org/10.1016/j.solmat.2020.110645.

Abdelrazik, A.; Osama, A.; Allam, A.N.; Shboul, B.; Sharafeldin, M.A.; Elwardany, M.; Masoud, A.M., (2023). ANSYS-Fluent numerical modeling of the solar thermal and hybrid photovoltaic-based solar harvesting systems. J. Therm. Anal. Calorim., 148: 11373–11424. https://doi.org/10.1007/s10973-023-12509-2.

Abdullah, A.; Atallah, F.S.; Ahmed, O.; Daoud, R., (2022). Performance improvement of photovoltaic/Trombe wall by using phase change material: Experimental assessment. J. Energy Storage, 50: 104194. https://doi.org/10.1016/j.est.2022.105596.

Al Arni, S., Mahdi, J. M., Abed, A. M., Hammoodi, K. A., Hasan, H. A., Homod, R. Z., & Khedher, N. B. (2024). Novel multi-layer nano-modified PCM configuration for efficient thermal management of photovoltaic-thermal systems. Journal of Energy Storage, 103, 114352. https://doi.org/10.1016/j.est.2024.114352.

Alikhan, A.H.; Kazemi, M.; Soroush, H., (2023). Enhanced performance of photovoltaic thermal module and solar thermal flat plate col-

lector connected in series through integration with phase change materials. Therm. Sci. Eng. Prog., 39: 101661. https://doi.org/10.1016/j.tsep.2023.102305.

Al-Karboly, A. M., Ibrahim, A., Fazlizan, A., Sopian, K., Al-Aasam, A. B., Ishak, M. A. A. B., ... & Elmnifi, M. (2025). Experimental evaluation of a photovoltaic thermal collector using twisted tape absorber with nano-enhanced phase change material for thermal storage. Journal of Energy Storage, 109, 115122. https://doi.org/10.1016/j.est.2024.115122.

Asefi, G., Ma, T., & Wang, R. (2022). Parametric investigation of photovoltaic-thermal systems integrated with porous phase change material. Applied Thermal Engineering, 201, 117727. https://doi.org/10.1016/j.applthermaleng.2021.117727.

Bhakre, S.S.; Sawarkar, P.; Kalamkar, V., (2023). Numerical study on photovoltaic thermal phase change material system in hot climatic conditions. Appl. Therm. Eng., 221: 119856. https://doi.org/10.1016/j.applthermaleng.2023.120423.

Deka, M.; Kamble, A.; Das, D.; Sharma, P.; Ali, S.; Kalita, P.; Bora, B.J.; Kalita, P., (2024). Enhancing the performance of a photovoltaic thermal system with phase change materials: Predictive modelling and evaluation using neural networks. Renew. Energy, 213: 118334. https://doi.org/10.1016/j.renene.2024.120091.

Jamil, F.; Ahmad, A.; Iqbal, M.; Khan, R., (2021). Evaluation of photovoltaic panels using different nano phase change materials and a concise comparison: An experimental study. Renew. Energy, 169: 1265–1279. https://doi.org/10.1016/j.renene.2021.01.089.

Jeddi Farzane, O.; Daryani, S.; Mokhberkia, M.M., (2017). Explanation of urban development pattern in order to sustainable development. Int. J. Urban Manag. Energy Sustain., 1(3): 8–16. https://doi.org/10.22034/ijumes.2017.18.12.019.

Kumar, P. M., Karthick, A., Richard, S., Vijayakumar, M., Stalin, P. M. J., Kumar, D. G., ... & Eswarlal, V. K. (2021). Investigating performance of solar photovoltaic using a nano phase change material. Materials Today: Proceedings, 47, 5029-5033. https://doi.org/10.1016/j.matpr.2021.04.615.

Rad, M. A. V., Kasaeian, A., Mousavi, S., Rajaee, F., & Kouravand, A. (2021). Empirical investigation of a photovoltaic-thermal system with phase change materials and aluminum shavings porous media. Renewable Energy, 167, 662-675. https://doi.org/10.1016/j.renene.2020.11.135.

Rahimi, M., Azimi, N., Nouira, M., & Shahsavar, A. (2023). Experimental study on photovoltaic panels integrated with metal matrix sheets and bio-based phase change materials. Energy, 262, 125371. https://doi.org/10.1016/j.energy.2022.125371.

Rajamony, R.K.; Pandey, A.; Sofiah, A.; Paw, J.K.; Suraparaju, S.K.; Fatehmulla, A.; Chopra, K.; Samykano, M.; Farade, R.A., (2025). Experimental investigation of carbon-based nano-enhanced phase change materials assimilated photovoltaic thermal system. J. Taiwan Inst. Chem. Eng., 150: 105445. https://doi.org/10.1016/j.est.2024.111373.

Safavi, B., & Shojaeebagheinee, D. (2019). The Use of Photovoltaic Energy for Sustainable Urban Development Emphasizing economic and Environmental Considerations. International Journal of Urban Management and Energy Sustainability, 1(1), 71-85.https://dx.doi.org/10.22034/ijumes.2017.06.15.009.

Salimi Gargari,R , Mofidi Shemirani,S M and Sanaieian,H . (2025). Impact of Thermal Insulation on Energy Behavior of Residential Building Envelopes (Tehran's District 15). International Journal of Urban Management and Energy Sustainability, 6(4), 248-259.https://doi.org/10.22034/ijumes.2025.2060021.1311.

Sharaf, M.; Ali, A.; El-Shazly, A., (2022). Performance enhancement of photovoltaic cells using phase change material (PCM) in winter. Alex. Eng. J., 61(6): 4229–4239. https://doi.org/10.1016/j.aej.2021.09.044.

Tariq, I.; Hu, J.; Chen, W.; Wang, X.; Yan, Y., (2024). Thermal performance of ethylene tetrafluoroethylene foils integrated photovoltaics with phase change materials for building envelopes. Sol. Energy, 267: 112083. https://doi:10.1016/j.

solener.2024.112623.

Yu, Q., Chen, X., & Yang, H. (2021). Research progress on utilization of phase change materials in photovoltaic/thermal systems: A critical review. Renewable and Sustainable Energy Reviews, 149, 111313. https://doi.org/10.1016/j.rser.2021.111313.

Zhao, J., Ma, T., Li, Z., & Song, A. (2019). Year-round performance analysis of a photovoltaic panel coupled with phase change material. Applied energy, 245, 51-64. https://doi.org/10.1016/j.apenergy.2019.04.004.

Ziari, K.; Nezami, M., (2020). Assessment of effective measures in residential buildings for photovoltaic-systems installation (Case study: Ekbatan residential complex, Tehran, Iran). Int. J. Urban Manag. Energy Sustain., 2(2): 1–17. https://ijumes.com/article_242512.html.

HOW TO CITE THIS ARTICLE

Ranjbar Zeinali,M and Eghbali,S R . (2026). Enhancing the Energy Efficiency of Photovoltaic Panels by Using Phase Change Materials: An Experimental Study. (e738225). International Journal of Urban Management and Energy Sustainability, (), e738225

DOI: 10.22034/ijumes.2026.2069892.1327